Preprints of the 19th World Congress
The International Federation of Automatic Control
Cape Town, South Africa. August 24-29, 2014

Fault Tolerant Control for an Electric 4WD Vehicle's Path Tracking with Active Fault Diagnosis ⋆

Xian Zhang * **Vincent Cocquempot** *

* *LAGIS, Automatic Control Laboratory, Lille* 1 *University of Sciences and Technology, 59655, France (e-mail: xian.zhang@ed.univ-lille1.fr, vincent.cocquempot@univ-lille1.fr).*

Abstract: This paper investigates the path tracking problem for an electric vehicle which has four electromechanical wheel systems under normal and faulty conditions. With considering wheel slip constraints and certain actuator faults, a passive fault-tolerant controller based on variable structure control is developed to maintain the system stability and guarantee the acceptable tracking performance. Then based on the designed controller, a simple active fault diagnosis approach is introduced for this typical over-actuated system to isolate and evaluate faults more precisely. With the diagnosed information, an accommodated fault tolerant controller is designed to maintain the tracking performance. Finally, simulations of traction engine multiple faults are conducted to illustrate the proposed method.

1. INTRODUCTION

The four-wheels driving (4WD) electrical vehicle (EV), a typical overactuated system, reveals high potentials for path tracking performance in critical situations, see Vissers [2005]. However, the increased system complexity and number of actuators also increase the probability of fault occurrences, such as loss of steering, loss of traction of wheels... Fault-tolerant control (FTC) methods have been proposed for this overactuated EV system, see Yang et al. [2008]-Wang [2011]. Yang et al. proposed a hybrid FTC Scheme with a classical LQ optimal controller in Yang et al. [2008]-Yang et al. [2010], considering reducing the cost of the fault tolerant process, however the fault detection and isolation (FDI) approach was not presented.

For the control allocation or fault accommodation for 4WD EV, the key problem is to distinguish which wheel is healthy and which is faulty. In Casavola [2008] and Dumont [2006], an adaptive actuator allocation method based on an online parameter estimator and a control system reconfiguration strategy was proposed. However, for the four-wheels independently-driven vehicle, the driving wheels on the same side have the same effect on the vehicle's motion, it is hard to distinguish which one is faulty. In Wang [2011], the authors proposed a simple active fault diagnosis approach to isolate the faults, this approach should be based on a controller that can guarantee the system's stability all the time. Compared with those active FT controllers, passive approaches still take an important place for certain critical faults because they do not require the exact fault information given by FDI when applying the control law, see Wang [2011].

In addition to the actuator failure, control for vehicle to track a desired path without tire-road friction saturation is also another practical issue that should be considered, see Fu [2008]-Peng [2007]. Due to the physical characteristics of the vehicle, when the magnitude of the wheel slip reaches its limit, any further increase may lead to skipping which can cause system instability. Some researches have been conducted on speed limits and constrained trajectory problems for EV. In Leith [2005], a robust controller is designed in order to reduce the effects of the saturation of the rear steering actuators. In Peng [2004] and Potluri [2013], the authors present a control scheme for 4WS EV path tracking problem subject to wheel slip constraint, but the faulty situation is not considered.

Few studies consider the fault tolerant control design problem for 4WD EV with input saturation. This FTC problem with considering input limitations was investigated in many other application fields, such as the spacecraft attitude system in aeronautics: in Guan [2008], an adaptive FT controller with actuator saturation is provided; in Huo [2011] and Hu [2011], the authors design a variable structure FT controller subject to input saturation which shows effectiveness for the spacecraft attitude systems.

Based on the existing researches, this paper investigates the problem of fault tolerant path-tracking control with input saturation for 4WD EV. A passive fault-tolerant control scheme based on variable structure control is developed to maintain the system stability and guarantee acceptable tracking performance in faulty situation. Based on the designed controller, a simple active fault diagnosis approach is introduced for this typical over-actuated system to isolate and evaluate faults more precisely. With the diagnosis information, an accommodated controller is designed to maintain better tracking performance.

The remainder of this paper is organized as follows. Section II describes the system model of 4WD EV to be coped with. Section III presents a simplified mathematical model. Fault case and input saturation problems are presented in Section IV. Section V proposes the variable-structure FTC

⋆ This work was supported in part by China Scholarship Council.

design. In Section VI, based on the simple active fault diagnosis method, the new controller is implemented to compensate the degraded performance. Finally in Section VII, the effectiveness of the proposed method is shown through simulations of traction engine multiple faults in driving situation.

2. SYSTEM MODELING

The EV is presented in Fig. 1. It has four actuated wheels and two actuated steering systems. Motor part is defined by 4DC traction motors, delivering a relative important mass torque. Front and rear steering motions are obtained through 2DC actuators, see Chatti [2013].

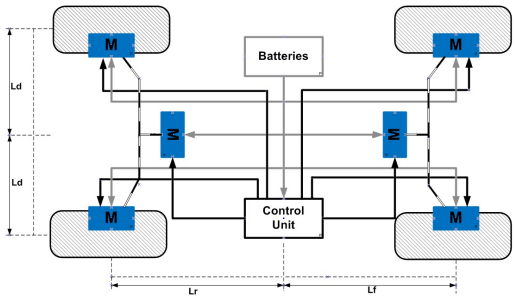

Fig. 1. The Ev's schematic diagram

Fig. 2 describes the three features of EV, namely, vehicle body, four wheels and the reference path for tracking. The state variables are: the center of gravity(CG) speed $\nu = \|V\|$, the sideslip angle β , the yaw rate γ , the perpendicular distance y_c , the angle ϕ between the vehicle velocity and the tangent to the path curve, and the wheel angular speeds $\omega_i(\ i = 1, 2, 3, 4)$.

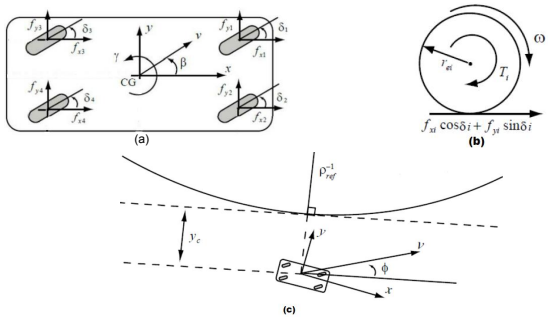

Fig. 2. (a)Vehicle body (b)Wheel model (c)Path-tracking kinematics

The dynamical equations of the three subsystems can be expressed as follows, see Peng [2004],Peng [2007] and Chen [2012]:

2.1 Vehicle body

$$\begin{bmatrix} m & 0 & 0 \\ 0 & m\nu & 0 \\ 0 & 0 & J_z \end{bmatrix} \frac{d}{dt} \begin{bmatrix} \nu \\ \beta \\ \gamma \end{bmatrix} = \begin{bmatrix} \cos\beta & \sin\beta & 0 \\ -\sin\beta & \cos\beta & 0 \\ 0 & 0 & 1 \end{bmatrix} \sum_{i=1}^{4} \begin{bmatrix} f_{xi} \\ f_{yi} \\ M_{zi} \end{bmatrix} + \begin{bmatrix} -\sigma_{aero}\nu^2 \cos\beta \\ \sigma_{aero}\nu^2 \sin\beta - m\nu\gamma \\ 0 \end{bmatrix} \quad (1)$$

where m is the mass of the vehicle, f_{xi} and f_{yi} are traction forces which are mainly result from the tire-road frictions, σ_{aero} stands for the aerodynamical coefficient, M_{zi} is the yaw moment and has the following form

$$\sum_{i=1}^{4} M_{zi} = \begin{bmatrix} -L_d & L_f \end{bmatrix} \begin{bmatrix} f_{x1} \\ f_{y1} \end{bmatrix} + \begin{bmatrix} L_d & L_f \end{bmatrix} \begin{bmatrix} f_{x2} \\ f_{y2} \end{bmatrix} + \begin{bmatrix} -L_d & -L_r \end{bmatrix} \begin{bmatrix} f_{x3} \\ f_{y3} \end{bmatrix} + \begin{bmatrix} L_d & -L_r \end{bmatrix} \begin{bmatrix} f_{x4} \\ f_{y4} \end{bmatrix} \quad (2)$$

where L_d is one half of the distance of the tread and L_f, L_r are the distances between the center of gravity and the front axle and the rear axle, see Fig. 1.

2.2 Wheel Model

$$I_{wi} \frac{d}{dt} \omega_i = T_i - r_{ei} \begin{bmatrix} \cos\delta_i & \sin\delta_i \end{bmatrix} \begin{bmatrix} f_{xi} \\ f_{yi} \end{bmatrix} \quad (3)$$

where I_{wi} is the inertia of the wheel, r_{ei} is the wheel's radius, δ_i is the steering angle and T_i is the wheel torque.

2.3 Path-tracking kinematics

$$\dot{y_c} = -\nu \sin\phi \quad (4)$$

$$\dot{\phi} = -\nu\rho_{ref} \cos\phi + \dot{\beta} + \gamma \quad (5)$$

where ρ_{ref} is the tangent to the path curvature.

2.4 Wheel Slip Constraint

The combined wheel slip S_i consists of two elements: the longitudinal slip S_{Li} and the lateral slip S_{Si}, see Fig. 3.

$$S_i = \begin{bmatrix} S_{Li} \\ S_{Si} \end{bmatrix} = \frac{1}{max(r_{ei}\omega_i \cos\alpha_i, \|V_i\|)} \begin{bmatrix} r_{ei}\omega_i \cos\alpha_i - \|V_i\| \\ r_{ei}\omega_i \sin\alpha_i \end{bmatrix} \quad (6)$$

where α_i presents the slip angle, β_i the sideslip angle of each wheel and $\|V_i\|$ the velocity of each wheel center.

The tire-road friction coefficient, depending on $\|S_i\|_2$ and road condition χ, is defined as $\mu_{Res}(\|S_i\|_2, \chi)$. It directs in the same direction with $\|S_i\|_2$. In this paper, it uses the model in Kiencke [1994]

$$\mu_{Res}(\|S_i\|_2) = \mu_0 \|S_i\|_2 / (a\|S_i\|_2^2 + b\|S_i\|_2 + 1) \quad (7)$$

Obviously it satisfies the following features:

$$\mu_{Res}(\|S_i\|_2)_{\|S_i\|_2=0} = 0, \quad \left.\frac{\partial \mu_{Res}(\|S_i\|_2)}{\partial \|S_i\|_2}\right|_{\|S_i\|_2=0} \triangleq k_i \quad (8)$$

where the initial slop k_i depends mainly on road conditions. A better road condition provides a higher initial slop and in turn gives a larger friction coefficient, see Peng [2004].

The friction forces (f_{xi}, f_{yi}) are defined as

$$\begin{bmatrix} f_{xi} \\ f_{yi} \end{bmatrix} = f_{zi} \begin{bmatrix} \cos\beta_i & -\sin\beta_i \\ \sin\beta_i & \cos\beta_i \end{bmatrix} \begin{bmatrix} 1 & 0 \\ 0 & k_{si} \end{bmatrix} \frac{\mu_{Res}(\|S_i\|_2)}{\|S_i\|_2} \begin{bmatrix} S_{Li} \\ S_{Si} \end{bmatrix} \quad (9)$$

where f_{zi} is the dynamical normal load and k_{si} the tire-tread-profile attenuation factor of each wheel.

In theory, if the magnitude of $\|S_i\|_2$ exceeds the threshold related to road condition, so does the friction force in Eq. (9). Conversely, if $\|S_i\|_2$ is limited, the saturation of friction force can be avoided.

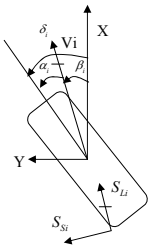

Fig. 3. Angles and slips for the i-th wheel

3. SIMPLIFIED MODEL

In most of the control researches for vehicle control, two common assumptions are presented at the control design stage and all give acceptable results: the absence of slip angle and the free rolling condition. Based on the two assumptions, a linearized tire model can be obtained from Eq. (3) as in Peng [2004]:

$$(\frac{I_{wi}\nu_0}{r_{ei}^2 k_i f_{zsi}})\frac{d}{dt}\partial\omega_i = -\partial\omega_i + \frac{1}{r_{ei}}(\partial\nu + (-1)^i \gamma L_d) + \frac{\nu_0}{r_{ei}^2 k_i f_{zsi}} T_i \quad (10)$$

where $\partial\omega_i = \omega_i - \omega_{i0}$, $\partial\nu = \nu - \nu_0$, f_{zsi} is the static normal load having the following form

$$f_{zs} = \frac{mg}{2}[\frac{L_r}{L_f+L_r} \quad \frac{L_r}{L_f+L_r} \quad \frac{L_f}{L_f+L_r} \quad \frac{L_f}{L_f+L_r}]^T \quad (11)$$

Because the eigenvalue of the wheel subsystem $r_{ei}^2 k_i f_{zsi}/I_{wi}\nu_0$ is quite large in comparison to that of the other two subsystems, it can be concluded that the wheel subsystem converges much faster, see Chen [2012]. Hence, based on the singular perturbation theory, the wheel subsystem can be replaced by its quasi-steady approximation.

When the wheel subsystem starts close to the steady state, the quasi-steady combined wheel slip is given as

$$\tilde{S}_i = \begin{bmatrix} \dfrac{T_i}{r_{ei} f_{zsi} k_i} \\ -\beta - \dfrac{l_i}{\nu_0}\gamma + \delta_i \end{bmatrix} \quad (12)$$

where $l_1 = l_2 = L_f$, $l_3 = l_4 = -L_r$.

Then around $\|V_0\| = \nu_0$, $\beta_0 = 0$, $\gamma_0 = 0$, $y_{c0} = 0$, $\phi_0 = 0$, the following linearized system for (1)-(5) is obtained:

$$\dot{x} = \begin{bmatrix} -2\sigma_{aero}\nu_0/m & 0 & 0 & 0 & 0 \\ 0 & \sigma_{aero}\nu_0/m & -1 & 0 & 0 \\ 0 & 0 & 0 & 0 & 0 \\ 0 & 0 & 0 & 0 & -\nu_0 \\ 0 & \sigma_{aero}\nu_0/m & 0 & 0 & 0 \end{bmatrix} x$$

$$+ \begin{bmatrix} 1/m & 0 & 0 \\ 0 & 1/m\nu_0 & 0 \\ 0 & 0 & 1/J_z \\ 0 & 0 & 0 \\ 0 & 1/m\nu_0 & 0 \end{bmatrix} \sum_{i=1}^{4} \begin{bmatrix} f_{xi} \\ f_{yi} \\ M_{zi} \end{bmatrix} + \begin{bmatrix} -\sigma_{aero}\nu_0^2/m \\ 0 \\ 0 \\ 0 \\ -\nu_0\rho_{ref} \end{bmatrix} \quad (13)$$

where $x = [\partial\upsilon \ \beta \ \gamma \ y_c \ \phi]^T$ are the measurable states.

And the forces and yaw moments are obtained from Eq. (9) and Eq. (12):

$$\begin{bmatrix} f_{xi} \\ f_{yi} \\ M_{zi} \end{bmatrix} = \begin{bmatrix} 1 & 0 \\ 0 & 1 \\ l_{1i} & l_{2i} \end{bmatrix} \begin{bmatrix} f_{zsi}k_i & 0 \\ 0 & k_{si} f_{zsi} k_i \end{bmatrix} \tilde{S}_i \quad (14)$$

where $l_{11} = l_{13} = -L_d$, $l_{12} = l_{14} = L_d$, $l_{21} = l_{22} = L_f$, $l_{23} = l_{24} = -L_r$.

4. CONTROL SCHEME

In order to avoid friction saturation, $\tilde{S}_i$ should be limited. By combining Eq. (13) and Eq. (14), the path-tracking control for 4WD EV is transferred to a problem of state regulation subject to input constraints. Choosing $\tilde{S}_i$ as the control signals that should be designed, based on Eq. (12), the wheel torque T_i and wheel steering δ_i are derived as

$$\begin{bmatrix} T_i \\ \delta_i \end{bmatrix} = \begin{bmatrix} \tilde{r_e} f_{zsi} \tilde{k} & 0 \\ 0 & 1 \end{bmatrix} \left(\begin{bmatrix} 0 \\ \beta + \dfrac{l_i \gamma}{\nu_0} \end{bmatrix} + \begin{bmatrix} u_i \\ u_{\delta i} \end{bmatrix} \right) \quad (15)$$

where $\tilde{r_e}$, $\tilde{k}$ are the estimated effective radius, slop of Eq. (8). Since the front and rear wheels on the same side have the same effect on the vehicle yaw and longitudinal motion, see Wang [2011],Peng [2004],Chen [2012], for simplification, we assume that the combined wheel slips on the same side are supposed to be identical, i.e. $u_1 = u_3 = u_l$, $u_2 = u_4 = u_r$ and $u_{\delta 1} = u_{\delta 3} = u_{\delta l}$, $u_{\delta 2} = u_{\delta 4} = u_{\delta r}$.

Let consider the traction engine actuator fault gain $0 \le f_i \le 1$. It means that the actual applied torques are

$$T_{fi} = f_i T_i \quad (16)$$

where $f_i = 1$ in no fault situation, $f_i < 1$ presents the loss of control effectiveness while $f_i = 0$ the complete failure.

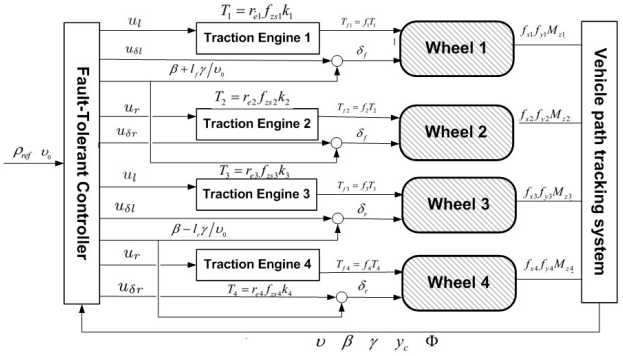

Fig. 4. The complete control scheme

Let substitute Eq. (15) into Eq. (14) and Eq. (13) with assumption that all four wheels have the same radius, attenuation factor and initial slop, and let $\tilde{k_s}$ be the estimated attenuation factor in Eq. (9), then the system can be represented as

$$\dot{x} = Ax + B_f(I_4 + \Delta_b)u + d = Ax + BF(I_4 + \Delta_b)u + d \quad (17)$$

where $\Delta_b = \mathbf{diag}\{(\tilde{r_e} - r_e)/r_e, (k_s k - \tilde{k_s}\tilde{k})/(\tilde{k_s}\tilde{k}), (\tilde{r_e} - r_e)/r_e, (k_s k - \tilde{k_s}\tilde{k})/(\tilde{k_s}\tilde{k})\}$ and $(\tilde{r_e}, \tilde{k_s}, \tilde{k})$ are chosen to satisfy $\tilde{r_e}\tilde{k} \le r_e k$, $\tilde{k_s}\tilde{k} \le k_s k$, $\tilde{r_e} \ge r_e$ to make Δ_b positive or semi-positive. The other matrices in Eq. (17) are defined just below.

Fig. 4 shows the complete control scheme.

As mentioned before, the wheel slip should be limited to avoid friction saturation, therefore the following assumption of input constraints is made.

Assumption 1. Let us assume that the control signals to the motor's driver are limited, that is,

$$|u_i| \le u_{max} \quad and \quad |u_{\delta i}| \le u_{max} \quad i = 1, 2, 3, 4 \quad (18)$$

where the chosen criterion of u_{max} is related to the physic of tire and its limit of the wheel slip.

Based on the given assumption and the system model, the objective is to design a fault-tolerant

$$A=\begin{bmatrix}-2\sigma_{aero}\nu_0/m & 0 & 0 & 0 & 0\\ 0 & \sigma_{aero}\nu_0/m & -1 & 0 & 0\\ 0 & 0 & 0 & 0 & 0\\ 0 & 0 & 0 & 0 & -\nu_0\\ 0 & \sigma_{aero}\nu_0/m & 0 & 0 & 0\end{bmatrix}, d=\begin{bmatrix}-\sigma_{aero}\nu_0^2/m\\ 0\\ 0\\ 0\\ -\nu_0\rho_{ref}\end{bmatrix}, u=\begin{bmatrix}u_l\\ u_{\delta f}\\ u_r\\ u_{\delta r}\end{bmatrix}$$

$$B=\begin{bmatrix}\frac{(f_{zs1}+f_{zs3})\tilde{k}}{m} & 0 & \frac{(f_{zs2}+f_{zs4})\tilde{k}}{m} & 0\\ 0 & \frac{\tilde{k_s}(f_{zs1}+f_{zs3})\tilde{k}}{m\nu_0} & 0 & \frac{\tilde{k_s}(f_{zs2}+f_{zs4})\tilde{k}}{m\nu_0}\\ \frac{-l_d(f_{zs1}+f_{zs3})\tilde{k}}{J_z} & 0 & \frac{l_d(f_{zs2}+f_{zs4})\tilde{k}}{J_z} & 0\\ 0 & 0 & 0 & 0\\ 0 & \frac{\tilde{k_s}(f_{zs1}+f_{zs3})\tilde{k}}{m\nu_0} & 0 & \frac{\tilde{k_s}(f_{zs2}+f_{zs4})\tilde{k}}{m\nu_0}\end{bmatrix}, F=\begin{bmatrix}\frac{f_{zs1}f_1+f_{zs3}f_3}{f_{zs1}+f_{zs3}} & 0 & 0 & 0\\ 0 & 1 & 0 & 0\\ 0 & 0 & \frac{f_{zs2}f_2+f_{zs4}f_4}{f_{zs2}+f_{zs4}} & 0\\ 0 & 0 & 0 & 1\end{bmatrix} \quad (17)$$

controller for system Eq. (17) to achieve path tracking mission, with considering faults in the traction engines, and input saturation to avoid the tire-road friction saturation problem.

5. VARIABLE STRUCTURE FAULT TOLERANT CONTROLLER DESIGN

Consider the vehicle tracking along a path of curvature ρ_{ref} with a constant speed v_0. The control objective is

$$x_d=[\partial v_d\ \ \beta_d\ \ \gamma_d\ \ y_{cd}\ \ \phi_d]^T=[0\ \ 0\ \ v_0\rho_{ref}\ \ 0\ \ 0]^T$$

For the steady states above, when applying the control, we can have the constant solution Γ for

$$Ax_d+B\Gamma+d=0 \quad (19)$$

It will yield:

$$\begin{cases}\frac{(f_{zs1}+f_{zs3})\tilde{k}\Gamma_l}{m}+\frac{(f_{zs2}+f_{zs4})\tilde{k}\Gamma_r}{m}-\frac{\sigma_{aero}\nu_0^2}{m}=0\\ \frac{\tilde{k_s}(f_{zs1}+f_{zs2})\tilde{k}\Gamma_{\delta l}}{m\nu_0}+\frac{\tilde{k_s}(f_{zs2}+f_{zs4})\tilde{k}\Gamma_{\delta r}}{m\nu_0}-\nu_0\rho_{ref}=0\\ -\frac{l_d(f_{zs1}+f_{zs3})\tilde{k}\Gamma_l}{J_z}+\frac{l_d(f_{zs2}+f_{zs4})\tilde{k}\Gamma_r}{J_z}=0\end{cases} \quad (20)$$

With considering faults based on Eq. (20), one obtains

$$\begin{cases}2\tilde{k}\Gamma_{lf}(f_{zs1}f_1+f_{zs3}f_3)=\sigma_{aero}\nu_0^2\\ 2\tilde{k}\Gamma_{rf}(f_{zs2}f_2+f_{zs4}f_4)=\sigma_{aero}\nu_0^2\end{cases} \quad (21)$$

Noted that in Eq. (21), $f_1(orf_2)$ and $f_3(orf_4)$ are all in the denominator of the fraction of Γ, they can not be 0 at the same time. The estimated lateral friction forces in Eq. (20) can be as $\Gamma_{\delta l}=\Gamma_{\delta r}=m\nu_0^2\rho_{ref}/(\tilde{k_s}\tilde{k}\sum_{i=1}^{4}f_{zsi})$, according to the dynamics theory, the maximum lateral friction forces should be greater than the centrifugal force to achieve a cornering motion in a constant speed v_0 with curvature ρ_{ref}, see Peng [2004] and Peng [2007], therefore one has

$$u_{max}>\tilde{\sigma}=\max\{\Gamma_l,\Gamma_r,\Gamma_{\delta l},\Gamma_{\delta r}\} \quad (22)$$

Let $e=x\quad x_d$, the dynamical error equation for system Eq. (17) can be obtained as

$$\dot{e}=Ae+B[(I_4+\Delta_b)Fu-\Gamma] \quad (23)$$

where the pair (A,B) is controllable.

Introducing the integral compensation $z=[z_1\ \ z_1\ \ z_3]$ to eliminate steady-state error, see Peng [2007], where $\dot{z}=[\partial v\ \ \beta\ \ y_c]$, we can get the following augmented system

$$\dot{\eta}=\tilde{A}\eta+\tilde{B}[(I_4+\Delta_b)Fu-\Gamma] \quad (24)$$

where

$$\eta=\begin{bmatrix}e\\ z\end{bmatrix}\quad \tilde{A}=\begin{bmatrix}A & 0_{5\times3}\\ C & 0_{3\times3}\end{bmatrix}, \tilde{B}=\begin{bmatrix}B\\ 0_{3\times4}\end{bmatrix}\quad C=\begin{bmatrix}1&0&0&0&0\\0&1&0&0&0\\0&0&0&1&0\end{bmatrix}$$

For Eq. (24), a passive fault-tolerant controller based on variable structure method is designed. Firstly, consider the following manifold:

$$s=\eta \quad (25)$$

Secondly, a fault tolerant controller based on variable structure is proposed in Huo [2011] and Hu [2011]:

$$u=-\frac{u_{max}\tilde{B}'P}{\|\tilde{B}P\|}\bar{s} \quad (26)$$

where $P=P'>0_{8\times8}$, the vector $\bar{s}$ has elements $\bar{s_i}, i=1,2,...,8$. The ith element has the following form

$$\bar{s_i}=\frac{s_i}{|s_i|+\delta} \quad (27)$$

where δ is a positive constant to be chosen.

Theorem 1. Let P be a positive symmetric matrix which is the solution of the following Riccati equation:

$$P\tilde{A}+\tilde{A}^TP-P\tilde{B}\tilde{B}'P+\varepsilon I_8=0 \quad (28)$$

With the given u_{max}, the designed controller (26) can guarantee the stability of the faulty path tracking control system for the states in $L_v(\mu)$, where

$$L_v(\mu)=\{\eta:\eta^TP\eta\le\mu\}\quad with\quad |\eta_i|\le c_i \quad (29)$$

with condition that

$$\lambda_{fj}\ge\frac{\prod_{i=1}^{8}\hbar_i}{\hbar_{min}}\left(\frac{\|\tilde{B}'P\|}{u_{max}}+\frac{\Gamma_j\|\tilde{B}'P\|}{u_{max}\|\tilde{B_j}'P_i\eta\|}\right) \quad (30)$$

where λ_{fj} is the relative eigenvalue of F, $\hbar_i=|\eta_i|+\delta$ and $\hbar_{min}=\min_{i=1,2,3,...,8}\{\hbar_i\}$.

Proof. Choose a Lyapunov function as

$$V=s^TPs=\eta^TP\eta \quad (31)$$

By computing the derivative of Eq. (31) and substituting Eq. (24)- Eq. (28), one can get

$$\begin{aligned}\dot{V}&=\dot{\eta}^TP\eta+\eta^TP\dot{\eta}\\ &=\eta^T(\tilde{A}^TP+P\tilde{A})\eta+2\eta^TP\tilde{B}Fu+2\eta^TP\tilde{B}\Delta_bFu-2\eta^TP\tilde{B}\Gamma\\ &=-\varepsilon\eta^T\eta-\eta^TP\tilde{B}\tilde{B}'P\eta+2\eta^TP\tilde{B}\tilde{B}'P\eta-2\eta^TP\tilde{B}\Gamma\\ &\quad -2\eta^TP\tilde{B}F\frac{u_{max}\tilde{B}'P}{\|\tilde{B}'P\|}\bar{s}-2\eta^TP\tilde{B}\Delta_bF\tilde{B}'P\frac{u_{max}}{\|\tilde{B}'P\|}\bar{s}\end{aligned}$$

Defining $u_L=-\tilde{B}'P\eta$, $\dot{V}$ becomes

$$\begin{aligned}\dot{V} &= -\varepsilon\eta^T\eta - \eta^T P\tilde{B}\tilde{B}'P\eta + 2u_L'u_L + 2u_L F\frac{u_{max}\tilde{B}'P}{\|\tilde{B}'P\|}\bar{s} \\ &\quad +2u_L\Gamma - 2\eta^T P\tilde{B}\Delta_b F\tilde{B}'P\frac{u_{max}}{\|\tilde{B}'P\|}\bar{s} \\ &\leq -\varepsilon\eta^T\eta - \eta^T P\tilde{B}\tilde{B}'P\eta + 2u_L'u_L - 2\frac{\hbar_{min}}{\prod_{i=1}^{8}\hbar_i}u_L'F\frac{u_{max}u_L}{\|\tilde{B}'P\|} \\ &\quad +2|u_L|\Gamma - 2\eta^T P\tilde{B}\Delta_b F\tilde{B}'P\frac{u_{max}}{\|\tilde{B}'P\|}\bar{s} \\ &= -\varepsilon\eta^T\eta - \eta^T P\tilde{B}\tilde{B}'P\eta - 2\eta^T P\tilde{B}\Delta_b F\tilde{B}'P\frac{u_{max}}{\|\tilde{B}'P\|}\bar{s} \\ &\quad +2\sum_{j=1}^{4}(u_{Lj}^2 - \lambda_{fj}\frac{\hbar_{min}}{\prod_{i=1}^{8}\hbar_i}\frac{u_{max}u_{Lj}^2}{\|\tilde{B}'P\|} + |u_{Lj}|\Gamma_j)\end{aligned}$$

Since Δ_b is chosen to be positive or semi-positive, then

$$-2\eta^T P\tilde{B}\Delta_b F\tilde{B}'P\frac{u_{max}}{\|\tilde{B}'P\|}\bar{s} \leq 0$$

If $(u_{Lj}^2 - \lambda_{fj}\frac{\hbar_{min}}{\prod_{i=1}^{8}\hbar_i}\frac{u_{max}u_{Lj}^2}{\|\tilde{B}'P\|} + |u_{Lj}|\Gamma_j) \leq 0$, i.e,

$$\begin{aligned}\lambda_{fj} &\geq \frac{\prod_{i=1}^{8}\hbar_i}{\hbar_{min}}\frac{(|u_{Lj}| + \Gamma_j)\|\tilde{B}'P\|}{u_{max}|u_{Lj}|} \\ &= \frac{\prod_{i=1}^{8}\hbar_i}{\hbar_{min}}(\frac{\|\tilde{B}'P\|}{u_{max}} + \frac{\Gamma_j\|\tilde{B}'P\|}{u_{max}|u_{Lj}|})\end{aligned}$$

Then we can have $\dot{V} \leq 0$.

Notice that with the saturated input, $|u_{Lj}|$ can't reach infinity. Assuming that the controller reaches its limit, $\dot{V}$ will become

$$\begin{aligned}\dot{V} &\leq -\varepsilon\eta^T\eta - \eta^T P\tilde{B}\tilde{B}'P\eta - 2\eta^T P\tilde{B}\Delta_b F\tilde{B}'P\frac{u_{max}}{\|\tilde{B}'P\|}\bar{s} \\ &\quad +2\sum_{j=1}^{4}|u_{Lj}|(|u_{Lj}| - \lambda_{fj}^{max}u_{max} + \Gamma_j)\end{aligned}$$

Here, λ_{fj}^{max} represents the fault gain of each actuator that the system can tolerate when input reaches its limits. Only λ_{fj}^{max} satisfies

$$\lambda_{fj}^{max} \geq \frac{|u_{Lj}|}{u_{max}} + \frac{\Gamma_j}{u_{max}}$$

can guarantee the system's stability under inputs saturation situation, that is to say, if $\lambda_{fj}^{max} = 1$, then any extra fault will destroy the stability, hence one has

$$\frac{|u_{Lj}|}{u_{max}} + \frac{\Gamma_j}{u_{max}} \leq 1$$

i.e.

$$|u_{Lj}| \leq \|\tilde{B_j}'P_i c\| \leq u_{max} - \Gamma_j \tag{32}$$

where c has elements c_i defined as the region of stability of our system in Eq. (29).

Remark 1. The designed controller (26) satisfies the input saturation limits, that is

$$|u_i| = |-\frac{u_{max}\tilde{B_j}'P_i}{\|\tilde{B}P\|}\bar{s}_i| \leq u_{max}$$

Remark 2. Obviously in practical situation, the designed passive fault-tolerant controller with input constraints cannot handle all faults. If the performance of the tracking system degrades out of the stability region, it's better to suspend the vehicle.

6. ACTIVE FAULT DIAGNOSIS

The designed passive FTC can guarantee the stability and some performance, possibly degraded, for the expected faults.

After t_f the actuator faults occur, the control matrix $\tilde{B}$ changes to $\tilde{B}_f$. In the practical situation, if the performance degradation is over the acceptable requirements but still within stability region, in order to eliminate the degradation, the control law should be changed to

$$u = -\frac{u_{max}\tilde{B_f}'P_f}{\|\tilde{B_f}P_f\|}\bar{s} \tag{33}$$

where P_f is the solution of

$$P_f\tilde{A} + \tilde{A}^T P_f - P\tilde{B_f}\tilde{B_f}'P + \varepsilon I_8 = 0 \tag{34}$$

There are three time instants that should be considered, see Yang et al. [2008]:

$[0, t_f]$: system is controlled by controller (26)

$(t_f, t_d]$: the faults are diagnosed and the parameters of controller (33) are calculated, system is still controlled by controller (26)

(t_d, ∞): system is controlled by the accommodated controller.

When referring to the fault diagnosis, since both wheels on the same side are all driving wheels, with only the measurable states applied by system (17), it is hard to distinguish which one is faulty. In Wang [2011], the authors proposed a simple active diagnosis method that is to actively change the motor control gain by virtually multiplying the motor control signal by a positive value. We will adopt this method to explicitly localize the faulty wheel and estimate the control gains.

For the healthy system and the faulty ones, based on Eq. (20), the following equations hold:

$$\begin{aligned}&(f_{zs1}f_1 + f_{zs3}f_3)u_{lf} + (f_{zs2}f_2 + f_{zs4}f_4)u_{rf} \\ &\quad = (f_{zs1} + f_{zs3})u_{lh} + (f_{zs2} + f_{zs4})u_{rh}\end{aligned} \tag{35}$$

where the subscripts h, f represent respectively the healthy system and the faulty one. As the traction engine actuator fault gain f_i changes in Eq. (35) when a fault happens, we will have a simple fault detection law as

$$\begin{cases} u_j = u_{jh} & no\ fault\ happens \\ u_j \neq u_{jh} & faults\ happen \end{cases}$$

with j presents the left or the right side.

It can be seen that f_1, f_3, f_2, f_4 are all unknown in the above Eq. (35), so virtual faults should be added to obtain other equations to solve these unknown parameters. As the motor control gain can be changed by multiplying the control signal by positive values κ_1 , κ_2, κ_3 and κ_4, after the additional faults are added, one has

$$\begin{aligned}&(\kappa_1 f_{zs1}f_1 + \kappa_3 f_{zs3}f_3)u_{l_{f\kappa}} + (f_{zs2}f_2 + f_{zs4}f_4)u_{r_{f\kappa}} \\ &\quad = (f_{zs1} + f_{zs3})u_{lh} + (f_{zs2} + f_{zs4})u_{rh}\end{aligned} \tag{36}$$

where $\kappa_1 \neq \kappa_3$. Based on Eq. (35) and Eq. (36), we can get the value of f_1 and f_3 separately. Using the same principle, by adding $\kappa_2, \kappa_4 (\kappa_2 \neq \kappa_4)$, we can also get the value of f_2 and f_4.

Remark 3. Although in Eq. (36) we multiply the control signal by a positive value κ, if the virtual fault gains can not make the EV system reach out of its stability region, for the designed FTC, κ will be treated as a new actuator fault gain of the traction engine, therefore the FTC designed in the previous section can make sure the stability of our system even when the additional virtual fault is added.

7. SIMULATIONS

The numerical example is presented by using MATLAB.

The parameters of the friction coefficient $\mu_{Res}(\|S_i\|_2, \chi)$ in Eq. (6) are chosen as: $\mu_0 = 28.6, a = 35, b = 1$. The parameters and the reference path are given in Table. 1, the constraint of $\|S_i\|_2$ is chosen as 0.025, the condition Eq. (22) is satisfied.

The vehicle starts with the initial states: $\nu(0) = 30 m/s, \beta(0) = 0\, rad, \gamma(0) = 0\, rad/s, y_c(0) = 10\, m, \phi(0) = 0\, rad, \omega_i(0) = 85.7\, rad/s$. The aerodynamical coefficient σ_{aero} is chosen as $0.445 kg/m$. In order to make Δ_b positive or semi-positive, we choose $\tilde{r_e} = 0.37, \tilde{k_s} = 0.85, \tilde{k} = 20.047$ to get

$$\Delta_b = diag\{0.0571, 0.5106, 0.0571, 0.5106\}$$

Table. 1 Parameters and the reference path

Parameter	Value
m(kg)	350
$l_f(m)$	0.401
$l_r(m)$	0.802
$l_d(m)$	0.605
$r_{ei}(m)$	0.350
$I_{\omega i}(kg \cdot m^2)$	0.7
$J_z(kgm^2)$	82
$v_0(m/s)$	30
$\rho_{ref}(m^{-1})$	1/40000
k_s	0.9
k	28.6

Substituting these parameters into system (24), we can obtain

$$B = \begin{bmatrix} 98.3305 & 0 & 98.3305 & 0 \\ 0 & 2.786 & 0 & 2.786 \\ -253.9206 & 0 & 253.9206 & 0 \\ 0 & 0 & 0 & 0 \\ & 2.786 & 0 & 2.786 \end{bmatrix}$$

Choosing $\varepsilon = 4.26 \times 10^{-3}, \delta = 2 \times 10^{-3}$, P, see Eq. (37) can be obtained by using function *care*. Based on Theorem. 1, the degradation of ν should not be over 0.5 m/s, then the free-rolling condition and linearized Eq. (13) can hold.

The faults are a lost of effectiveness of traction engines. The nominal gain of each engine is set to 10 seconds, then two faults are introduced: the gain of front-left is reduced to $f_1 = 0.5$, and rear-left to $f_3 = 0.5$.

From Fig. 5 we can see that before $10s$ the system with the proposed controller is stable and shows good performance, and after faults happen, the controller is able to keep the system's stability. However, as the other states reaching to the objective, ν and β still have errors with the desired values, see Fig. 6.

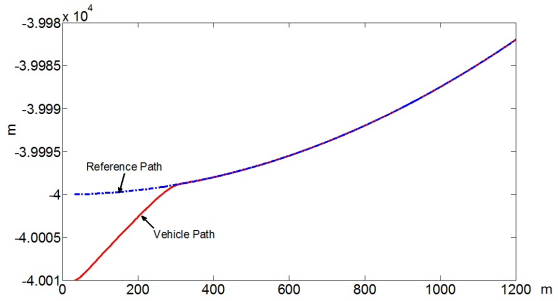

Fig. 5. Tracking result

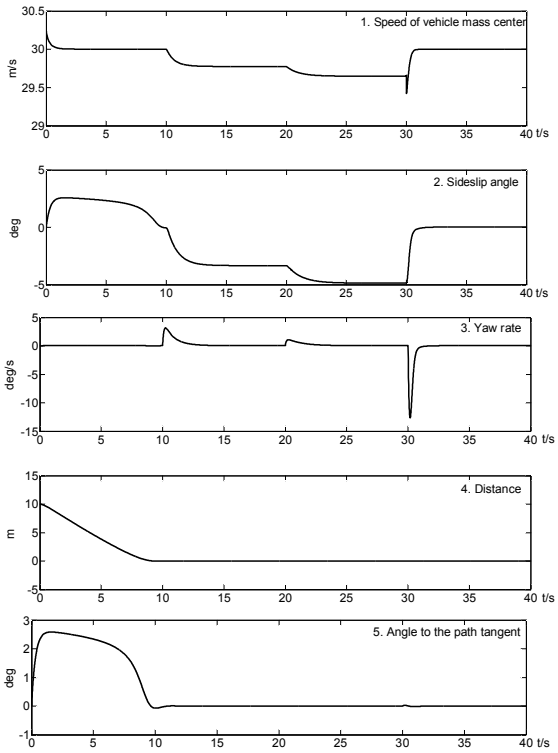

Fig. 6. (1) Speed of vehicle mass center ν; (2) Side slip angle β; (3) Yaw rate γ; (4) Distance y_c; (5) Angle ϕ

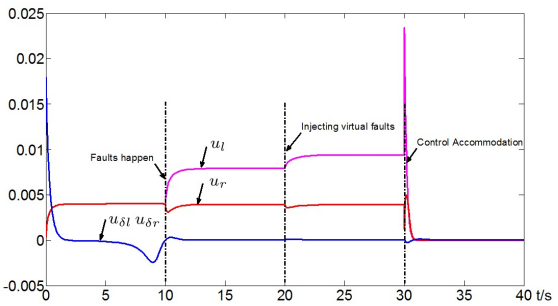

Fig. 7. Control signals with active fault diagnosis

Therefore, at $20s$ we add the virtual faults $\kappa_1 = 0.9$, $\kappa_3 = 0.7$. At $30s$, the virtual faults are cancelled.

With the data of control signals we collect in Fig. 7, we can calculate that $\hat{f}_1 = 0.43$ and $\hat{f}_3 = 0.55$. Here for simplification we omit the part to get $\hat{f}_2$ and $\hat{f}_4$.

After detecting the faults and estimating the fault gains, the controller (33) with P_f can be applied at $30s$. From

$$P = \begin{bmatrix} 0.0005 & 0 & 0 & 0 & 0 & 0.0005 & 0 & 0 \\ 0 & 0.0078 & -0.0003 & -0.0002 & 0.0068 & 0 & 0.0045 & 0.0001 \\ 0 & -0.0003 & 0.0002 & 0 & -0.0002 & 0 & -0.0001 & 0 \\ 0 & 0.0002 & 0 & 0.0034 & -0.024 & 0 & 0.0002 & 0.0026 \\ 0 & -0.0068 & -0.0002 & -0.024 & 0.30021 & 0 & -0.0038 & -0.0161 \\ 0.0005 & 0 & 0 & 0 & 0 & 0.0047 & 0 & 0 \\ 0 & 0.0045 & -0.0001 & 0.0002 & -0.0038 & 0 & 0.0075 & 0.0001 \\ 0 & 0.0001 & 0 & 0.0026 & -0.0161 & 0 & 0.0001 & 0.0064 \end{bmatrix} \quad (37)$$

Fig. 6 we can see that the new controller can eliminate the performance degradation.

8. CONCLUSIONS

With considering wheel slip constraints and certain actuator faults, a FTC based on variable structure control is developed. Based on the designed controller, a simple active fault diagnosis (AFD) approach is introduced for this typical overactuated system to isolate and evaluate faults precisely. With the diagnosis information, the accommodated controller is generated. However, the whole process works only when the system is still within the region of stability, when to execute AFD, what is the influence of the virtual faults to the system and how to guarantee the accuracy of AFD... are still need to be studied, therefore the work in the future will focus on supplying a complete FTC scheme to solve these problems.

REFERENCES

J. P. M. Vissers. The control design for an overactuated vehicle. *Theis of Technische Universiteit Eindhoven*, Eindhoven, August 2005.

H. Yang, V. Cocquempot and B. Jiang. Hybrid fault tolerant tracking control design for electric vehicles. *16th Mediterranean Conference on Control and Automation Congress Centre*, Ajaccio, France, June 25-27 2008.

H. Yang, V. Cocquempot and B. Jiang. Optimal fault tolerant path tracking control for 4WD4WS electric vehicle. *IEEE Transaction on Intelligent Transportation Systems*, 11(1):237–243 2010.

A. Casavola and E. Garone. Enhancing the actuator fault tolerance in autonomous overactuated vehicles via adaptive control allocation. *the 5th International Symposium on Mechatronics and Its Applications*, pages 1–6, May 27-29 2008.

P. E. Dumont, A. Aitouche, R. Merzouki and M. Bayart. Fault tolerant control on an electric vehicle. *IEEE International Conference on Industrial Technology*, pages 2450–2455, Dec 15-17 2006.

R. Wang and J. M. Wang. Fault-tolerant control with active fault diagnosis for four-wheel independently-driven electric ground vehicles. *2011 American Control Conference on O'Farrel Street*, San Francisco, CA, USA, June 29 - July 01 2011.

R. Wang and J. M. Wang. Passive fault-tolerant control of a class of over-actuated nonlinear systems and applications to electric vehicles. *2011 50th IEEE Conference on Decision and Control and European Control Conference(CDC-ECC)*, Orlando, FL, USA, December 12-15 2011.

L. Fu and U. Ozguner. Sliding mode in constrained source tracking with non-nolonomic vehicles. *International Workshop on Variable Structure Systems(VSS '08)*, Antalya, June 8-10 2008.

R. Potluri and A. K. Singh. Path-tracking control of an autonomous 4WS4WD electric vehicle using its natural feedback loops. *2013 IEEE Multi-conference on System and Control (Conference on Control Applications)*, Hyderabad, India, August 28-30 2013.

R. Potluri and A. K. Singh. Path-tracking control of an autonomous 4WS4WD electric vehicle using driving motors' dynamics. *Proceedings of the 7th IEEE International Conference on Industrial and Information Systems (ICIIS)*, pages 1–2, Indian Institute of Technology Madras, Chennai, India, 2012.

D. J. Leith and M. Vilaplana. Robust lateral controller for 4-wheel steer cars with actuator constraints. *Proceedings of the 44th IEEE Conference on Decision and Control and the European Control Conference 2005*, Seville, Spain, December 12-15 2005.

S. T. Peng, J. J. Sheu and C. C. Chang. A control scheme for automatic path tracking of vehicle subject to wheel slip constraint. *Proceeding of the 2004 American Control Conference*, pages 804–809, Bonston, Massachusetts, June 30 - July 2 2004.

S. T. Peng. On one approach to constraining the combined wheel slip in the autonomous control of a 4WS4WD vehicle. *IEEE Transaction on Control System Technology*, 15(1):168–175, 2007.

W. Guan and G. H. Yang. Adaptive fault tolerant control of linear systems in the presence of actuator saturation and L2 disturbances. *Proc.20th Chinese Control and Decision Conference*, Yantai, China 2008.

X. Huo, Q. L. Hu, B. Xiao and G. F. Ma. Variable-structure fault tolerant attitude control for flexible satellite with input saturation. *Control Theory and Application*,28(9):1063–1068, 2011.

Q. L. Hu, B. Xiao and M. I. Friswell. Robust fault-tolerant control for spacecraft attitude stabilisation subject to input saturation. *IET Control Theory Appl.*,5(2):271–282, 2011.

N. Chatti, A.L. Gehin, O.B. Belkacem, and R. Merzouki. Functional and behavior models for the supervision of an intelligent and autonomous system. *IEEE Transaction on Automation Science and Engineering*,10(2):431-445, April, 2013.

C.F. Chen, Y.M. Jia, J.P. Du and F.S. Yu. Lane keeping control for autonomous 4WS4WD vehilecs subject to wheel slip constraint. *2012 American Control Conference*, Fairmont Queen Elizabeth, Montral, Canade, June 27 - 29 2012.

U. Kiencke and A. Daiβ. Estimation of tyre friction for enhanced ABS-system. *Proceedings of the International Symposium on Advanced Vehicle Control 1994 (AVEC'94)*,pages 515–520, Tokyo, Japan 1994.